Simultaneous Quantification of Imidacloprid and its Metabolites in Tissues of Mice upon Chronic Low-dose Administration of Imidacloprid

Collins NIMAKO[1], Yoshinori IKENAKA[1,2,8,9], Osei Akoto[3], Kazutoshi FUJIOKA[4], Kumiko TAIRA[5], Koji ARIZONO[6], Keisuke KATO[7], Keisuke TAKAHASHI[7], Shouta M.M. NAKAYAMA[1], Takahiro ICHISE[1] and Mayumi ISHIZUKA[1]

[1]Laboratory of Toxicology, Department of Environmental Veterinary Sciences, Faculty of Veterinary Medicine, Hokkaido University, Japan.
[2]Water Research Group, Unit for Environmental Sciences and Management, North-West University, Potchefstroom, South Africa
[3]Chemistry Department, Kwame Nkrumah University of Science and Technology, Ghana
[4]Pharmaceutical Research Institute, Albany College of Pharmacy and Health Sciences
[5]Department of Anesthesiology, Tokyo Women's Medical University Center east, Tokyo, Japan
[6]Faculty of Environmental and Symbiotic Sciences, Prefectural University of Kumamoto, Kumamoto, Japan
[7]Faculty of Pharmaceutical Sciences, Toho University, 2-2-1 Miyama, Funabashi, Chiba, 274-8510, Japan
[8]Translational Research Unit, Veterinary Teaching Hospital, Faculty of Veterinary Medicine, Hokkaido University, Japan
[9]One Health Research Center, Hokkaido University, Japan

*Corresponding Author: Yoshinori IKENAKA

Faculty of Veterinary Medicine, Hokkaido University, Kita 18, Nishi 9, Kita-ku, Sapporo, Hokkaido 606-0818, Japan

Tel : +81-11-706-6949

Fax : +81-11-706-5150

E-mail: y_ikenaka@vetmed.hokudai.ac.jp

Abstract

This study aimed to (i) develop a sensitive method for simultaneous detection and quantification of imidacloprid (IMI) and seven of its metabolites in tissue specimens, and to (ii) determine the biodistribution of the IMI compounds in tissues of C57BL/6J male mice; after exposure to 0.6 mg/kg bw/day of IMI (10% of no observable adverse effect level of IMI) through a powdered diet for 24 weeks. We successfully developed a method which was accurate (recoveries were ≥ 70% for most compounds), sensitive (LODs ≤ 0.47 ng/mL and LOQs ≤ 1.43 ng/mL were recorded for all detected compounds, $R^2 \geq 0.99$) and precise (RSDs ≤ 20%) for routine analysis of IMI and seven of its metabolites in blood and various tissue matrices. After bio-distributional analysis, IMI and five of its metabolites were detected in mice. Brain, testis, lung, kidney, inguinal white adipose tissue and gonadal white adipose tissue mainly accumulated IMI, blood and mesenteric white adipose tissue mainly accumulated IMI-olefin; liver mainly accumulated desnitro-IMI; pancreas predominately accumulated 4-hydroxy-IMI. The desnitro-dehydro-IMI and the desnitro-IMI metabolites recorded tissue-blood concentration ratios ≥ 1.0 for testis, brain, lung and kidney. The cumulative levels of the six detected IMI compounds (Σ6 IMI compounds) were found in the decreasing order: blood > testis > brain > kidney > lung > iWAT > gWAT > mWAT > liver > pancreas. Altogether, this study provided essential data needed for effective mechanistic elucidation of compound-specific adverse outcomes associated with chronic exposures to IMI in mammalian species.

Keywords: *Imidacloprid, IMI-olefin, 4-Hydroxy-IMI, N-Desnitro-IMI, 5-Hydroxy-IMI, N-Desnitro-4,5-dehydro-IMI.*

1. Introduction

Neonicotinoid insecticides (NNs) stand out as the world`s most favorite class of insecticides, used extensively for pest extermination in households, veterinary health care and in agriculture [1]. The global affection for NNs is largely ascribed to their competitive insecticidal potencies, low mammalian toxicity, broad insecticidal spectra, enhanced systemic properties and their high plant compatibilities [2,3,4]. Being neurotoxicants, NNs agonize the nicotinic acetylcholine receptors (nAChRs), expressed within the central nervous systems of both vertebrates and invertebrates [5]. They are known to be effective against different species of biting, chewing and sucking insects.

Imidacloprid (IMI; *1-(6-chloro-3-pyridylmethyl)-N-nitroimi-dazolidin-2-ylideneamine*; *Fig.1*) is one of the most popular NNs across the world; accounting for about 41.5% of the total neonicotinoid use in the world [2,6]. It is also labeled as the second most widely used insecticide worldwide; with an annual production estimate of 20000 tonnes [7]. As a result of the high global use of IMI, its residues are now pervasive in many environmental compartments. Several studies have detected high residual levels of IMI in environmental matrices such as soil, water, sediments and in human food [8,9,10,11]. Reports from biomonitoring studies have also indicated steady increases in IMI exposure trends among human populations worldwide [12,13,14,15,16,17].

Like other NNs, IMI was previously considered to be less toxic to mammalian species, due to its limited binding affinity for the mammalian nAChR. In recent times however, the advent of *in vivo* and *in vitro* studies has disputed this assumption, by revealing significant toxicological potencies of IMI on physiological functioning of key mammalian organs such

as brain [18,19], liver [20], adipose tissues [6], ovaries [21], heart and kidney [22]. From pharmacokinetic studies however, IMI is known to have a quick excretion rate in mammalian models (more than 90% of radiolabeled IMI was recovered in rats within 24 h after administration [23]). It is, therefore, perplexing whether the recent IMI-related toxicological outcomes observed in mammalian species are specifically induced by IMI itself or by any of its metabolites.

Following enteric absorption, IMI is transformed by phase I and phase II enzymes into various metabolite forms; and each of the metabolites tend to elicit different effects, affinities or potencies towards the nAChRs [2,3,24,25]. For instance, the olefin metabolite of IMI (4,5-dehydro-imidacloprid, IMI-olefin or IMI-ole) is known to be selectively toxic to insects than the parent IMI [25,26]. Also, the desnitro metabolite of IMI (*N*-desnitro-imidacloprid, dn-IMI) agonizes the mammalian nAChRs than the parent IMI compound [27,28]. Conceivably, an *in vivo* evaluation of tissue-specific accumulation trends of all the IMI-related compounds in mammalian species, may provide essential data needed for effective mechanistic elucidation of compound-specific adverse outcomes associated with chronic exposures to IMI in mammalian species.

Currently, information on the tissue-specific accumulation of IMI and its associated metabolites within the mammalian system is highly limited. So far, the only study cited in literature, used a single exposure assay to elucidate the tissue-specific distribution of some IMI-compounds in a lizard model [3]. However, the use of such a one-time exposure assay may not reveal the exact tissue-specific accumulation trends associated with chronic low-

dose exposures to IMI, as expected in real-life situations. Besides, a reptile model may not be suitable for efficient prediction of IMI distribution, accumulation and excretion in human systems; largely because of existing differences in the xenobiotic excretion pathways between humans (excretion occurs largely through urine and faeces) and reptiles (excretion occurs largely through molting). To this end, the use of a rodent model may offer a better alternative for extrapolating the biodistribution data of IMI into human situations. So far, only a handful of studies have reported on IMI metabolism and its tissue-dependent distribution in rodent models. However, almost all those studies focused on the excretion kinetics and transient tissue distribution patterns of IMI, rather than its long-term accumulation in tissues [26]. The lack of a long-term exposure-related tissue accumulation data on IMI throws a big challenge to scientific advances towards uncovering the mechanistic pathways that underlie the recent IMI-mediated adverse outcomes observed in mammalian models.

Determination and quantification of xenobiotics in biological specimens require a precise, reliable and accurate analytical method. Already, some few studies have succeeded in developing methods for imidacloprid analysis in biological specimens; however, those studies focused on urine specimen only [4,13,29]. Besides, all the published IMI-detection methods published were efficient for the detection of only few IMI-related compounds. So far, no method has been established for the simultaneous analysis of multiple IMI-related compounds in different kinds of tissue specimens.

116 Previously, Wang *et al.* [3] and Yang *et al. [30]* optimized an analytical protocol for
117 quantification of IMI and its metabolites in tissues of lizards. However, the protocol was
118 valid for only four IMI compounds. Also, Ford and Casida [31] published a detection
119 technique for quantification of IMI and its metabolites in tissues of mice, however, their
120 method was applicable to only brain and liver. Most of the published detection techniques of
121 IMI compounds [3, 30, 31] lacked robust purification systems. In those methods, tissue
122 extracts were injected directly into HPLC systems, after passing through membrane filters.
123 Due to the complexity of tissue matrices, the lack of appropriated clean-up procedures in
124 such analytical methods may present a considerable amount of matrix interference in tissue
125 analysis of IMI compounds. The incorporation of an SPE clean up procedure in the current
126 method will offer an optimum accuracy for routine analysis of multiple IMI compounds in
127 various tissue specimens.

128 This study aimed to (i) develop rugged, robust and sensitive SPE (solid phase extraction) and
129 LC-MS/MS-based technique for simultaneous detection and quantification of IMI and its
130 metabolites (IMI compounds) in tissues, and to (ii) determine the tissue-specific
131 accumulation trends of IMI and its related metabolites in tissues of C57BL/6J male mice,
132 after a long-term low dose exposure of IMI to the mice. A triple quadrupole LC-MS/MS
133 system was used for this study because of its high sensitivity, good accuracy, low limit of
134 detection (LOD) and low limit of quantification (LOQ).

135 ## 2. Materials and Methods

136 ### 2.1. Materials

137 Eight (8) IMI compounds; IMI, IMI-olefin, dn-IMI, 4-hydroxy-imidacloprid (4OH-IMI), 5-
138 hydroxy-imidacloprid (5OH-IMI), *N*-desnitro-4,5-dehydro-imidacloprid (dn-dh-IMI), 6-
139 chloronichotinic acid (6-CNA) and 6-chloronichotinic acid-glycine (6-CNA-glycine)
140 *(Fig.1)*; and two isotope-labelled internal standards; Imidacloprid-d4 (IMI-d4) and 6-
141 Chloronicotinoic acid-13C6 (6-CNA-13C6), were analyzed in the current study. The IUPAC
142 nomenclature, molar masses and CAS numbers of the target IMI compounds are presented
143 in *Table S2*. IMI was purchased from Kanto Chemical Co., Inc. (Chuo-Ku, Tokyo, Japan);
144 standards of 5OH-IMI, 4OH-IMI, 6-CNA-glycine, dn-IMI and dn-dh-IMI were synthesized
145 in Toho university (Chiba, Japan) [32, 33, 34]; 6-CNA standard was purchased from Wako
146 Pure Chemical Industries (Osaka, Japan); IMI-ole standard was obtained from Supelco
147 (USA); IMI-d4 and 6CNA-13C6 internal standards were purchased from Cambridge Isotope
148 Laboratories, Inc. (Tewksbury, MA, United States). Male C57BL/6J mice, aged 3 weeks
149 were obtained from Sakyo Labo Service Corporation, Inc. (Edogawa-ku, Tokyo, Japan).
150 Powdered diet (D12451M, with red dye) was purchased from Research Diets Inc. (New
151 Brunswick, NJ 08901, USA). All reagents and solvents used in the current study were of
152 HPLC grade; and they were purchased from Kanto Chemical Co., Inc. (Chuo-Ku, Tokyo,
153 Japan).

154 ### *2.2. In-vivo* protocol

155 This animal study was conducted in accordance with the Institutional Animal Care and Use
156 Committee of the Faculty of Veterinary Medicine, Hokkaido University, Japan. The animal
157 experiments were performed in accordance with the Guide for the Care and Use of

158 Laboratory Animals, in conformity with the Association for the Assessment and
159 Accreditation of Laboratory Animal Care International (AAALAC; approval number: 18-
160 0061; validity period: 04/2018 - 03/2023). The animal facility used for the present study was
161 controlled for temperature (20-25 ºC), humidity (40-60 ºC) and 12-hour light/dark cycle.
162 After 2 weeks of acclimatization, mice were divided into two groups (control-group and IMI-
163 exposed group; 4 mice per group). Mice in the IMI-exposed group were treated with 0.6
164 mg/kg bw/day of IMI (one-tenth of the NOAEL dose of IMI) through a powdered diet for 24
165 weeks. In the control-group, mice were provided with only powdered diet for the 24-week
166 period. In our previous study [20], a chronic (24 week) exposure to $1/10^{th}$ of the NOEAL of
167 IMI drastically altered the lipid homeostasis of mice. Also, Sun *et al. [6]* found out that an
168 exposure to $1/10^{th}$ of the NOAEL of IMI increases adiposity and alters glucose metabolism
169 in mice. Hence, $1/10^{th}$ of the NOAEL of IMI was selected for the current study due to its
170 toxicological significance to mammalian studies. In the present study, diet and water were
171 given to mice ad libitum throughout the experiment; and were provided fresh three times in
172 a week. At the end of the entire study, mice were sacrificed by CO_2 asphyxiation. At necropsy,
173 blood, lung, liver, testis, brain, kidney, pancreas inguinal white adipose tissue (iWAT),
174 mesenteric white adipose tissue (mWAT), and gonadal white adipose tissue (gWAT), were
175 collected and processed accordingly, for chemical analysis.

176 **2.3. Optimization of sample preparation method**

177 **2.3.1. Tissue extraction**

178 The tissue extraction method adopted in the current study was a modification of the protocol
179 published previously by Ohno *et al.* [35] and Nimako *et al.* [20]. The method optimization
180 process of the current study was carried out using mice brain that had undetected levels of
181 all the target chemicals (brain samples from mice in the control group). Specifically, a 10 -
182 15 mg blank brain tissue sample was spiked with 100 µL of IMI-internal standard master mix
183 containing 5 ng each of IMI-d4 and 6-CNA-13C6. The spiked tissue sample was
184 homogenized in 0.4 mL of 1% formic acid in acetonitrile, using Tissue Lyser (Qiagen GmbH,
185 Hilden, Germany). The homogenized tissue sample was mixed thoroughly by vortex; and
186 centrifuged at 10,000 G for 10 min. Following centrifugation, supernatant from the sample
187 (about 0.5 mL) was carefully separated into fresh 1.5 mL Eppendorf tube and labeled as SP1
188 (supernatant 1). The sample residue was subsequently reconstituted in 0.5 mL of methanol,
189 mixed thoroughly by vortex (2 min) and centrifuged again, at 10,000 G for 10 min.
190 Supernatant from the second extraction was carefully separated as before; and labeled as SP2
191 (supernatant 2). Both SP1 and SP2 were combined, mixed thoroughly to represent the final
192 tissue extract.

193 **2.3.2. Cleanup (Solid-Phase Extraction)**

194 A 0.2 mL of the tissue extract was diluted in 0.6 mL of 3% (v/v) methanol in distilled water
195 (HPLC grade). The diluted extract was purified with the InertSep CBA SPE cartridge (100
196 mg / 1 mL, GL Sciences, Tokyo, Japan), which contained a silica-based sorbent modified
197 with carboxyl ethyl functional groups. The cartridge was connected to the SPE manifold
198 (equipped with a vacuum pump), preconditioned with 2 mL methanol and dried under

vacuum for 10 min. The diluted tissue extract was loaded unto the pre-conditioned cartridge and allowed to elute at a rate of 1 mL/min. Eluate was collected into a pre-cleaned translucent test tube (15 mL) and labeled as F1 (fraction-one). The analytes were eluted from the cartridge into F1 with 1 mL of 20% (v/v) acetonitrile in distilled water (HPLC grade), at the same speed as stated previously. The eluate (F1) was evaporated to dryness under gentle stream of nitrogen gas at 60 ^{o}C. Finally, the dried sample was reconstituted in 0.2 mL of 20% (v/v) methanol in distilled water (HPLC grade), vortexed for 2 min and transferred into an LC vial for LC–MS/MS analysis.

The clean-up process of the brain tissue extracts was optimized by testing (I) three (3) additional SPE sorbents; thus, InertSep PSA cartridge (100 mg / 1 mL, GL Sciences, Tokyo, Japan), InertSep Pharma cartridge (60 mg / 3 mL, GL Sciences, Tokyo, Japan) and InertSep Phospholipid Remover (100 mg / 3 mL, GL Sciences, Tokyo, Japan); and (II) four different SPE elution solvents; thus, 20% (v/v) acetonitrile in distilled water, 50% (v/v) acetonitrile in distilled water, 20% (v/v) methanol in distilled water and 50% (v/v) methanol in distilled water, with the current method for optimal purification and elution efficiencies (n=3)

2.4. Instrumental analysis

The sample analysis was carried out using a triple quadrupole LC-/MS/MS system (Agilent 6495B, Agilent Co., CA, USA). The LC system (1290 Infinity II, Agilent) was equipped with a binary LC pump, a vacuum degasser, an autosampler and an oven. A gradient system of 0.1% formic acid + 10 mM ammonium acetate in; water (solvent A) and methanol (solvent B) were chosen for routines as follows: t = 0–1 min. 5% B (isocratic), t = 6 min: 95% B

(gradient), t = 6–8 min (gradient): 95% B (isocratic). The column oven temperature was set at 60 °C and the total mobile phase was pumped at a flow rate of 0.35 mL/min through a Kinetex Biphenyl column (2.1 mm ID ×150 mm, ø 1.7 µm; Phenomenex, Inc., CA, USA). The volume of each sample injected into the mobile phase flow was 10 µL.

The triple quadrupole mass spectrophotometer was equipped with an electrospray ionization (ESI) interface; the IMI compounds in the column eluents were quantified with a triple quadrupole mass filter. The sheath gas temperature and flow rate were 350 ^{o}C and 12 L/min respectively. The drying gas temperature, drying gas flow rate and nebulizer pressure were set at 210 ^{o}C, 17 L/min and 25 psi respectively. The capillary voltage was set at 3500 V for positive detection mode and 3000 V for the negative detection mode. The ion signals were acquired with multiple-reaction monitoring (MRM) in positive ionization mode; the selected m/z ions for the all the IMI compounds considered in the current study have been shown in *Table S1*. The MS/MS operating conditions were set in accordance with the manufacturer`s instructions and the data acquisition and processing were carried out using the MassHunter Workstation software (Agilent Technologies).

2.5. Method Validation

The current method was validated by evaluating method accuracy, matrix effects, linearity, inter-day and intra-day precisions, freeze-thaw stability, limit of detection (LOD) and the limit of quantification (LOQ). These quality assurance and quality control measures were adopted based on guidelines for method performance recommended by the SANTE standard (SANTE/11945/2019 [36]

241 Method accuracy was assessed by estimating the recoveries of matrix-matched standards of
242 the target chemicals. Blank brain tissues (obtained from the in-vivo experiment) were spiked
243 with working standard solutions containing all the target compounds and IMI internal
244 standards at 3 concentration levels; a low concentration (2.5 ng/mL; n=3), a medium
245 concentration (5.0 ng/mL; n=3) and a high concentration (10.0 ng/mL, n=3). In order to
246 normalize the influence of ME on method accuracy, recoveries of target chemicals that had
247 isotopically labelled standards (IMI and 6-CNA) were estimated by comparing analyte/IS
248 peak area ratios (37). Recoveries of target chemicals without internal standards were
249 estimated by comparing peak areas of matrix-matched standards to peak areas of post matrix-
250 matched standards.

251 Matrix effects were assessed by post-extraction matrix-spikes (tissue extracts were spiked
252 with 2.5 ng of the standard of each target compound, just before instrumental analysis); and
253 by comparing response of the target chemicals against response of their respective standards
254 prepared in 20% (v/v) MeOH in distilled water (n=3).

255 Linearity of the method was determined using matrix-matched calibration curves plotted
256 from nine different concentrations (0.03 to 21.87 ng/mL). The calibration plots were
257 subjected to linear regression analysis to obtain regression coefficients (r^2).

258 The LODs and LOQs were estimated from analysis of matrix matched standards as values at
259 which the signal-to-noise ratios were 3 and 10, respectively. The ratios of the analyte signal
260 to the noise in chromatogram were determined with the MassHunter Workstation software
261 (Agilent Technologies).

For Intra-day precision, blank brain samples were fortified with the target chemicals at 2.5, 5 and 10 ng/mL; and this was analyzed in five different batches (n=3). The inter-day precision was also examined at 5 ng/mL for 4 successive days (n=3, a single measurement per day). Both intra-day and inter-day precisions were estimated as percent standard deviations (% RSD; [4]).

The freeze-thaw stabilities of the target IMI compounds were evaluated according to the method described previously by Ueyama et al. [37].

2.6. Method variability

To ascertain conditions that may affect variability of the current method, we evaluated the relative instrumental response of the target IMI compounds in each of the following steps (I) three different tissue weights (10 mg, 20 mg and 50 mg) were tested to validate the tissue weight-dependency of the method accuracy, (II) eight different biological matrices (blood, brain, white adipose tissue, liver, lung, testis, pancreas and kidney) were tested with the method to evaluate the effects of matrix variability on the method accuracy (n=3).

2.7.Application of method for tissue distribution analysis of imidacloprid compounds

Following the 24-week IMI exposure, blood, liver, testis, brain, kidney, pancreas and adipose tissues (including inguinal, mesenteric and gonadal white adipose tissues) were harvested from mice and stored at -20 ^{o}C until analysis. Tissue concentrations of IMI and its metabolites were determined by the method developed and optimized in the present study. Four (4) types of matrix-matched calibration curves were employed to quantify the target

chemicals in various tissue specimens. (I) Brain matrix-matched samples were used to quantify the IMI compounds in brain, adipose tissue, and liver (these matrices showed similar matrix effect tendencies the target chemicals), (II) Pancreas matrix-matched samples were used to quantify all compounds in pancreas, lung, and kidney (these matrices showed similar matrix effect tendencies the target chemicals), (III) Testis matrix-matched samples were used to quantify all compounds in testis, and (IV) Blood matrix-matched samples were used to quantify all compounds in blood.

2.8.Statistical Analysis

Data from the present study were statistically analyzed using JMP Pro13 (SAS institute, USA). The data from all the experimental groups were tested for normality using the Shapiro-Wilk test; and for homogeneity of variance using the Levene's test. Figures were plotted using JMP Pro13 or Microsoft excel 2016 (version: 16.0.12527.21378) 64-bit.

3. Results and Discussion

3.1.Optimization of SPE sorbents

Efficiencies of 5 SPE cartridges; cation exchange (InertSep SCX and InertSep CBA), anion exchange (InertSep PSA) and neutral (InertSep Pharma and InertSep Phospholipid Remover), were evaluated for purification of the target IMI compounds in tissue extracts; and the results have been shown in *Fig*.2. Purification efficiencies of the cartridges were evaluated based on recoveries and matrix effects (ME) obtained from analysis of matrix-matched standard solutions containing the target chemicals.

304 Of the 5 SPE cartridges tested, the InertSep CBA and InertSep Pharma recorded best
305 purification efficiencies for all the compounds (both cartridges had recoveries of more than
306 70% for all the target compounds). However, elution with InertSep Pharma cartridge
307 produced higher matrix effects for most target compounds (ME range; from -11% of dn-dh-
308 IMI to -96% of IMI), compared to that of InertSep CBA (ME ranged; -15% of dn-dh-IMI to
309 -51% of IMI-olefin). The PSA recorded good recoveries of more than 70% for six out of the
310 eight (6/8) compounds (ME ranged; -18% of dn-IMI to -66% of IMI-olefin), InertSep
311 Phospholipid Remover recorded recoveries above 70% for five out of the eight (5/8) target
312 compounds (ME ranged; -15% of dn-IMI to -75% of IMI), SCX recorded acceptable
313 recoveries (> 70%) for four out of eight (4/8) of the target compounds (ME ranged; 11% of
314 4OH-IMI to -39% of IMI)

315 Most NN parent compounds are hydrophilic and electrically neutral [4]. However, NN
316 metabolites may differ from parent compounds in terms of charge densities, largely because
317 of structural and functional differences. For instance, the 6-CNA metabolite of IMI is acidic
318 and hence, may assume anionic charges when ionized, but the parent IMI is neutral in
319 solutions. Due to possible charge differences between IMI and its metabolites, designing a
320 simultaneous purification technique for all the metabolites of IMI could be challenging.

321 In the present study, we employ an ion exchange SPE with a trapping strategy (reverse phase
322 SPE). We selected ion exchange SPE cartridges which had the potential to trap impurities,
323 while allowing the target chemicals to elute. Prior to sample elution however, the tissue

extracts were diluted in DW to reduce viscosity and to facilitate elution of analyte through the sorbents.

The InertSep CBA, a weak cation exchanger was highly effective in trapping most impurities; and this was evident in the relatively low matrix effects obtained in relation to the CBA elution. At the same time, CBA (weak cation exchanger) exhibited low binding affinity for the target IMI compounds; and this resulted in high accuracies for all the target compounds. In contrast, the strong cation exchanger, InertSep SCX, trapped four of the target compounds (dn-IMI, dn-dh-IMI, 4OH-IMI and 5OH-IMI) along with impurities. Perhaps, dn-IMI, dn-dh-IMI, 4OH-IMI and 5OH-IMI had high binding affinities for strong cation exchangers. As such, SCX was considered unsuitable for the trapping SPE strategy employed in the current method.

The anion exchanger (InertSep PSA) permitted the elution of majority of the compounds (6/8); however, 6-CNA and 6-CNA-glycine were trapped in PSA. The 6-CNA and its glycine conjugates have acidic functionalities; and hence may exhibit anionic tendencies in solutions. The PSA cartridge probably trapped these metabolites through anion exchange interactions.

Although the neutral cartridge, InertSep Pharma, had good elution for all the target compounds, the matrix effects obtained from its associated clean-ups were mostly higher than those of other cartridges. This suggests that the neutral cartridge, Pharma, had lower efficiency for trapping most impurities in tissue extracts; compared to the anion and cation exchange cartridges. InertSep Phospholipid Remover is highly selective for removal of phospholipids from tissue extracts; and this is helpful for minimizing ion suppression in

LC/MS/MS analysis. In the present study however, InertSep Phospholipid Remover was found to trap 4OH-IMI, 5OH-IMI and 6-CNA along with tissue phospholipids; and this probably resulted into low recoveries for these compounds. As a result of the selective binding affinities of Phospholipid Remover for the target IMI compounds, it was considered unsuitable for the current purification strategy.

3.2.Optimization of SPE elution solvents

Four aqueous organic solvents, thus; 20% (v/v) MeOH, 50% (v/v) MeOH, 20% (v/v) ACN and 50% (v/v) were tested to determine their elution efficiencies for the target IMI compounds, using the InertSep CBA and InertSep SCX cartridges (*Fig. S1*). Out of all the solvents tested, 20% (v/v) ACN and 50% (v/v) MeOH showed the highest elution efficiencies for the target compounds. In the current method however, 20% (v/v) ACN was considered most suitable for elution of the target compounds, due to its likelihood to present lesser matrix interferences in LC-MS/MS analysis, as compared to methanol. Phospholipids in tissue extracts are known to be less soluble in acetonitrile, compared to methanol; as a result, acetonitrile has been found to be more effective in reducing MS signals than methanol [38].

3.3. Method validation

3.3.1. Accuracy

Accuracy estimation at three concentration levels (2.5, 5 and 10 ng/mL) yielded recoveries of more than or equal to 70% for all the target compounds (*Fig.S2*). Moreover, all the target IMI compounds recorded recoveries within the range of 70 - 120% in all the mice tissues considered in the current study, except for lung (Fig 3A). According to the

366 SANTE/11945/2019 guidelines, method performance is deemed acceptable if mean
367 recoveries fall within the range of 70-120%, with an associated repeatability RSD ≤ 20%. By
368 inference, recoveries obtained in the current study are suggestive that, the current method
369 had appropriate accuracy for detection and quantification of the target IMI-compounds in
370 most tissues considered in the present study. In lung, dn-dh-IMI, IMI-olefin, 5OH-IMI and
371 6-CAN-glycine had recoveries of 49%, 49%, 65% and 66% respectively (Fig 3A), however
372 these recoveries were recorded with good precisions (RSD ≤ 20%). In exceptional cases, the
373 SANTE/11945/2019 guideline gives room for acceptance of recovery rates that are within
374 the range of 30-140% (thus; recovery rates outside the range of 70-120%), provided they are
375 consistent (RSD ≤ 20%). This suggests that the current method had acceptable accuracy for
376 quantification of dn-dh-IMI, IMI-olefin, 5OH-IMI and 6-CAN-glycine in lungs as well.

377 When different tissue weights (10, 20 and 50 mg) were tested with the current method,
378 recoveries of all the target compounds were consistently found within acceptable range (70-
379 120%), regardless of the weight considered (Fig. S3). However, ion suppressions of the target
380 compounds were found to increase with increasing tissue weights *(Fig. S3).* These suggests
381 that the current method may produce optimum accuracies with minimum interferences, when
382 tested with low amounts of tissue specimens.

383 **3.3.2. Precision**

384 The intra-day precision estimated from the fortified tissue samples at 2.5, 5 and 10 ng/mL
385 yielded RSDs ≤ 20% for all the target IMI compounds *(Table 1)*. Moreover, inter-day
386 precision analysis yielded RSDs < 20% for all the target chemicals *(Table 1)*. These results

suggest that the current method had high consistency for detection and quantification of majority of the IMI compounds considered in the present study.

Meanwhile, the freeze and thaw stability evaluation yielded RSDs ≤ 20% for IMI, IMI-ole, 5OH-IMI and 6-CNA-glycine; and RSDs ≥ 20% for dn-dh-IMI, dn-IMI, 4OH-IMI and 6-CNA *(Table 1)*. These suggest that, beside IMI, IMI-ole, 5OH-IMI and 6-CNA-glycine, other IMI compounds may not exude adequate stabilities when subjected to continuous freezing and thawing cycles. A chromatogram of tissue-fortified samples has been shown in *Figs.4.* The peaks of all the target IMI compounds were resolved; and they were without interferences.

3.3.3. Matrix Effect

In the current study, matrix effects (MEs) of the target compounds were evaluated in all tissues *Fig 3B.* From the results, dn-IMI and dn-dh-IMI were found with the least MEs in all the tissues (median MEs were -6.1% and -10.8% respectively). According to SANTE/11945/2019 guidelines, analytes with MEs (%) within the range of ±20% are less susceptible to interferences during LC-MS/MS analysis. This suggest that dn-IMI and dn-dh-IMI suffered from minimal matrix suppression; and hence can be quantified by solvent calibrations, via the current method. Other IMI compounds targeted in the current study recorded MEs beyond the range of ±20%. Median MEs of IMI, 6-CAN, IMI-olefine, 5OH-IMI, 4OH-IMI and 6-CNA-glycine recorded in all the target tissues were -27.0%, -30.0%, -33.5% -44.8%, -64.3% and -63% respectively. This suggests that, apart from dn-IMI and dn-dh-IMI, all the target IMI compounds suffered from matrix inhibition during the instrumental

analysis. Matrix effects in analytical measurements are mainly caused by ion suppression and ion enhancement [39]. According to Ly *et al.,* [39], matrix effects in LC-MS/MS are more dependent on co-eluting components rather than the properties of an analyte. Hence this may be minimized by employing either isotopically labeled standards, matrix matched calibration curves or sample dilution in analytical measurements [39, 40, 41]. In the current study, both isotopically labeled standards and matrix matched calibrations curves were employed to normalize MEs during instrumental analysis.

3.3.4. Linearity

Matrix-matched calibration curves were plotted for various IMI compounds within the calibration range of 0.03 to 21.87 ng/mL. Linear responses and correlation coefficients of the target IMI compounds have been shown in *Table 1*. Linearity was considered acceptable, if a response yielded correlation coefficient greater than or equal to 0.99 [40]. Results from the present study revealed regression coefficients that were greater than 0.99 for all the IMI compounds considered in this study. This means that the current method produced excellent linear relationships for all the IMI compounds considered in the present study.

3.3.5. LOD and LOQ determination

Based on the signal-to-noise ratios of the matrix-matched calibration standards, we evaluated the method LODs and LOQs for all the target IMI compounds; and the results have been shown in *Table 1.* The results indicate LODs ranging from 0.06 ng/mL to 0.47 ng/mL and LOQs ranging from 0.17 ng/mL to 1.43 ng/mL for the target IMI compounds. These results

give strong indication that the current method had high sensitivities towards the detection and quantification of all the IMI compounds considered in this study.

3.4. Tissue distribution/accumulation of IMI and its metabolites

We applied the method developed in the current study to determine the distribution/accumulation trends of IMI and its metabolites in blood and tissues of C57BL/6J male mice, following a 24-week exposure to a low dose (less than the NOAEL dose) of IMI (*Figs. 5 and 6A; Table S3*). The tissues, considered in the present study include lung, liver, kidney, brain, pancreas, testis, mesenteric white adipose tissue, inguinal white adipose tissue and gonadal white adipose tissue.

3.4.1. Biodistribution of IMI

The parent IMI compound was detected in blood and all the target tissues, except for the liver (*Fig.6A*). The blood and tissue accumulation trends of IMI was found in the decreasing order; Testis > blood > brain > lung > kidney > iWAT > gWAT > mWAT> pancreas > liver (*Fig. 5*). From pharmacokinetic studies, IMI is known to undergo rapid oral absorption in mammalian systems; with a consequential distribution of its residues into various organs and tissues [42]. Perhaps, IMI elicited a quick enteric absorption into blood; and this might have facilitated its distribution into the organs and tissues considered in the current study model. The testis-blood concentration ratio of IMI was 1.0 (Table 2), suggesting that the testis accumulated a significant amount of IMI in the current experimental model. Meanwhile, the tissue-blood concentration ratios of IMI obtained for the other target chemicals in tissues

were all below 1.0 (Table 2). This suggests that the tissue distributional patterns of IMI observed in the current mice model was mainly instigated by a high exchange of blood between the target organs.

The high IMI accumulation trend in testis observed in the current study agrees with findings from a previous study which demonstrated significant distribution of IMI residues within lizard gonads [3, 30]. However, the brain accumulation pattern of IMI observed in the current rodent model contradicts previous findings from a reptile model [3]. Whereas the current study revealed a significant accumulation levels of IMI in mice brains, findings from Wang *et al.*`s study [3] showed very low residual levels of IMI in brains of lizards, after a single oral exposure to IMI. This contrasting observation might be due to specie-specific differences.

In the present study, IMI was not detected in the liver of the exposed mice probably because of its rapid metabolic transformation within the liver. Wang *et al.,* [3] also detected very low residues of IMI in liver of lizards, following a one-time oral exposure to IMI. Meanwhile, the current experimental model recorded appreciable amounts of IMI in mice adipose tissues (iWAT, gWAT, mWAT, *Fig. 6A*). These observations indicate that, although IMI is less lipophilic, significant amount of its residues may remain distributed in various adipose depots within the mammalian system, especially under conditions of long-term persistent exposures. In contrast, Wang *et al* [3] detected insignificant levels of IMI in fat, following a single oral exposure of IMI to lizards. This contrasting observation was probably because of the short-term exposure duration employed in their study and/or because of species-specific differences.

3.4.2. Biodistribution of IMI metabolites

Imidacloprid is primarily metabolized in mammalian liver either by CYP450-mediated imidazolidine hydroxylation or via aerobic nitroreduction by the molybdo-flavoenzyme aldehyde oxidase (AOX) [4, 5 31, 43]. In the present study, key metabolites of IMI such as 4OH-IMI, 5OH-IMI, IMI-ole, dn-IMI and dn-dh-IMI were detected in blood and tissues of the IMI exposed mice (*Figs. 5 and 6A; Table S3*). IMI-ole occurred as the most predominant metabolite followed by 4OH-IMI, then dn-IMI, with 5OH-IMI and dn-dh-IMI being the least recalcitrant in the tissues *(Figs. 5)*.

3.4.2.1.Biodistribution of IMI metabolites within the hydroxylation pathway

The imidazolidine hydroxylation pathway is known to be more prolific in IMI metabolism; and its activation transforms IMI into more water-soluble moieties such as 4OH-MI and 5OH-IMI. In the present study, 4OH-IMI and 5OH-IMI metabolites were highly detected in blood, kidney, lung and testis, but their levels in liver were very low (*Fig. 5*). The momentous detection of 4OH-IMI and 5OH-IMI in the present study confirms the CYP450-mediated imidazolidine hydroxylation pathway as a prominent rout of IMI metabolism in mammalian species. Interestingly, very low residual amounts of 4OH-IMI and 5OH-IMI metabolites were detected in liver, compared to other tissues *(Figs. 5 and 6A)*. This tendency might be due to the spontaneous non-metabolic transformation of 4OH-IMI and 5OH-IMI into the IMI-ole metabolite.

Imidacloprid-olefin is a desaturated secondary metabolite of 4OH-IMI and 5OH-IMI; and it occurs as the commonest metabolite of IMI found in mammalian species [5, 25]. This

491 explains why IMI-ole was recalcitrant metabolite in blood and most tissues considered in the
492 present study (testis, brain, lung, iWAT, gWAT and mWAT*; Figs. 5 and 6A)*. Wang *et al* [3]
493 also found IMI-ole as the predominant metabolite of IMI in lizard tissues. In current
494 experimental model IMI-ole detected with the least concentration in liver (*Fig. 6A)*. This
495 might be due to the metabolic conversion of IMI-ole into dn-dh-IMI in the liver. The dn-dh-
496 IMI metabolite of IMI is considered as a terminal product of the IMI hydroxylation pathway,
497 which is formed as a result of hepatic nitroreduction of IMI-ole *(Fig. 1)*. The levels of dn-dh-
498 IMI in the liver was found to be far higher than its levels detected in all the other tissues *(Figs.*
499 *5 and 6A)*, confirming dn-dh-IMI as a terminal metabolite within the IMI hydroxylation
500 pathway. The dn-dh-IMI metabolite specifically accumulated in liver, lung, testis and kidney
501 of the current mice model (tissue to blood concentration ratios were 3.8, 3.1, 2.0 and 1.7
502 respectively, *Table 2*)

503 **3.4.2.2.Biodistribution of IMI metabolites within nitroreduction pathway**

504 Nitroreduction of IMI presents an alternative pathway for IMI metabolism in mammalian
505 species. Hepatic activation of this pathway by AOX triggers series of metabolic events which
506 eventually yields the dn-IMI metabolite of IMI [5, 31, 43]. In the present study, dn-IMI
507 showed significant accumulation in liver, brain, testis, lung and kidney of mice (tissue to
508 blood concentration ratios were 1.8, 1.5, 1.4, 1.3 and 1.2 respectively; *Table 2, Fig 5*). From
509 a toxicological point of view, the specific accumulation of dn-IMI in organs such as brain
510 and testis, generate serious concerns, in that, the dn-IMI metabolite is known to elicit a
511 nicotinic-type action, with a markedly higher toxicity to mammals than the parent IMI.

512 The dn-IMI metabolite is known to serve a major precursor for prominent IMI metabolites
513 such as 6-CNA and its glycine conjugates; thus, 6-CNA-glycine (*Fig.1,* [5]). In the current
514 study, the 6-CNA and 6-CNA-glycine were not detected in the mice model presumably
515 because of the limited feasibility of the nitroreduction metabolic pathway of IMI.

516 **3.4.3. Cumulative levels of IMI and its metabolites in mice tissues**

517 Total accumulation levels of the IMI compounds in mice tissues were estimated by the
518 summation of mean concentrations of all the detected IMI compounds (Σ6 IMI compounds)
519 in each tissue *(Fig.6B).* The cumulative levels of the target IMI compound (Σ6 IMI
520 compounds) in blood and tissues occurred in the decreasing order; blood > testis > brain >
521 kidney > lung > iWAT > gWAT > mWAT > liver > pancreas *(Fig.6B).* This result suggests
522 that organs such as testis, iWAT and kidney may be most susceptible to cumulative effects
523 of IMI and its metabolites, after a chronic low-dose exposure to IMI in mammalian species.

524 **3.4.4. Interplay between the current mice study and human studies**

525 Despite the widespread use of IMI, its detected levels in most human studies are relatively
526 low, compared to levels of other NNs reported in biomonitoring studies [17, 37, 44, 45, 46,
527 47, 48]. In a pharmacokinetic study, Harada *et al.* [29] detected only a small percentage of
528 IMI in human urine (about 12.7%), after intentional ingestion of micro doses of deuterium-
529 labeled IMI by human subjects. These observations suggest that, a greater proportion of IMI,
530 probably undergoes transformation into other metabolite forms in the human body. Results
531 from the present study has given a clear evidence that, most metabolites of IMI produced in
532 human system, may accumulate in different organs and tissues within the body.

Many biomonitoring studies have already detected IMI metabolites such as 5OH-IMI and 6-CNA in human urine [44, 45, 46, 47, 48, 49, 50]. However, the detection frequency of 5OH-IMI reported in human subjects was very low (about 19.7%) [44]. Similarly, the accumulation levels of 5OH-IMI detected in the present study were found to be relatively low, compared to the levels of most of the other IMI-compounds detected in the current experimental model.

Although 6-CNA has been detected in some human studies [45, 47, 49, 50], its accumulation levels in the current mice model were below LOQ. The inconsistency may be attributed to the species-difference in IMI metabolism. This, however, brings to bear, the limitations that might be associated with extrapolation of mice study to humans. Nonetheless, recent biomonitoring studies have suggested that the 6-CNA metabolite may not be a dependable biomarker of IMI exposure in mammalian species, due to its frequent occurrence in metabolic pathways of several chemicals, including IMI, ACE, THI, NIT and cycloxaprid [47].

Recently, Wang *et al.* [48] detected dn-IMI and IMI-ole in human urine with high detection frequencies, high concentrations, high specificities and good inter-day reliabilities. Based on these findings, Wang *et al.* [48] projected IMI-ole as potential biomarker of IMI exposure in human populations. In the present animal model, the IMI-ole metabolite of IMI was predominately detected in blood and most of the target tissues. This probably validated Wang *et al's* projection of IMI-ole as a potential marker of IMI exposures in human subjects.

4. **Conclusion**

554 We developed an accurate, precise and a sensitive LC-MS/MS-based method for routing
555 analysis of multiple IMI-related compounds in tissue specimens. We thence, applied the
556 method to determine the tissue-specific accumulation trends of IMI and its metabolites in
557 C57BL/6J male mice, following a long-term exposure to a less than the NOAEL (the no-
558 observed adverse-effect level) level) of IMI. To the best of our knowledge, this is the first
559 study to establish an analytical protocol for detection and quantification of multiple IMI
560 compounds in tissue specimens. Moreover, this study is the first to provide a basic tissue
561 distribution and/or accumulation data associated with chronic low-dose exposures to IMI in
562 mammalian species. In the current study, the Biodistributional trends IMI compounds in
563 organs such as the heart, adrenal glands, stomach, etc. were not elucidated. We therefore
564 recommend that further studies should be done to evaluate the fate of IMI in these organs,
565 under chronic low-dose exposure situation.

566

567 **Acknowledgement**

568 This work was supported by the Grants-in-Aid for Scientific Research from the Ministry of
569 Education, Culture, Sports, Science and Technology of Japan awarded to M. Ishizuka (No.
570 21H04919 and JPMXS0420100620), Y. Ikenaka (No. 18H0413208), N. Hoshi (No.
571 19H0427719), and T Hirano (No. JP19K19406). The contribution of the NWU-Water
572 Research Group is @@. This work was also supported by the foundation of JSPS Bilateral
573 Open Partnership Joint Research Projects (JPJSBP120209902) and the Environment
574 Research and Technology Development Fund (SII-1/3-2, 4RF-1802/18949907) of the
575 Environmental Restoration and Conservation Agency of Japan. We also acknowledge

576 financial support from the Soroptimist Japan Foundation, the Nakajima Foundation, the
577 Sumitomo Foundation, the Nihon Seimei Foundation, act beyond trust, the Japan Prize
578 Foundation, and Triodos Foundation. This research was also supported by JST/JICA,
579 SATREPS (Science and Technology Research Partnership for Sustainable Development; No.
580 JPMJSA1501). This work was supported by the World-leading Innovative and Smart
581 Education (WISE) Program (1801) from the Ministry of Education, Culture, Sports, Science,
582 and Technology, Japan. The funders had no role in study design, data collection and analysis,
583 decision to publish, or preparation of the manuscript.

584

585 **Disclaimer**

586 The authors declare no conflict of interest in the present study.

587 **Data Accessibility**

588 Data, associated metadata, and calculation tools are available by contacting the
589 corresponding author (y_ikenaka@vetmed.hokudai.ac.jp).

590

591 **References**

592 1. M. L. Eng, M. J. B. Stutchbury, A. C. Morrissey, A neonicotinoid insecticide reduces
593 fueling and delaysmigration in songbirds. *Sci.* 365(2019), 1177–1180.

2. A. Cardone, Imidacloprid induces morphological and molecular damages on testis of lizard (*Podarcis sicula*). *Ecotoxicology* (2015), 2494–105. doi 10.1007/s10646-014-1361-0
3. Y. Wang, Y. Hana, P. Xua, B. Guoa, W. Lia, X. Wang, The metabolism distribution and effect of imidacloprid in chinese lizards (*Eremias argus*) following oral exposure. *Ecotoxicol Environ Saf.* 165(2018),476-483.
4. M. Honda, R. Robinson, K. Kannan, A simple method for the analysis of neonicotinoids and their metabolites in human urine, *Environ. Chem.* (2019), https://doi.org/10.1071/EN18240
5. X. Wang, A. Anadon, W. Qinghua, F. Qiao, I. Ares, M-R. Martınez-Larranaga, Z. Yuan, M-A. Martınez, Mechanism of neonicotinoid toxicity: impact on oxidative stress and metabolism. *Annu. Rev. Pharmacol. Toxicol.* 58(2017),18.1–18.37.
6. Q. Sun, X. Xiao, Y. Kim, D. Kim, S. K. Yoon, M. J. Clark, P. Park, Imidacloprid promotes high fat diet-induced adiposity and insulin resistance in male C57BL/6J mice. *J. Agric. Food Chem.* 64(2016), 9293−9306. doi: 10.1021/acs.jafc.6b04322
7. N. Simon-Delso, V. Amaral-Rogers, L.P. Belzunces, J. M. Bonmatin, M. Chagnon, C. Downs, L. Furlan, D.W. Gibbons, C. Giorio, V. Girolami, D. Goulson, D. Kreutzweiser, C. H. Krupke, M. Liess, E. Long, M. McField, P. Mineau, E. A. Mitchell, C. A. Morrissey, D. A. Noome, L. Pisa, J. Settele, D. J. Stark, A. Tapparo, H. Van Dyck, J. Van Praagh, P. J. Van der Sluijs, R. P. Whitehorn, M. Wiemers, Systemic insecticides (neonicotinoids and fipronil): trends, uses, mode of action and

615 metabolites. *Environ. Sci. Pollut. Res. Int.* 22(2015), 5–34.
616 https://doi.org/10.1007/s11356-014-3470-y
617 8. D. A. E. Mitchell, B. Mulhauser, M. Mulot, A. Mutabazi, G. Glauser, A. Aebi1, A
618 worldwide survey of neonicotinoids in honey. *Sci.* 358 (2017), 109–111
619 9. C. Lu, C. Chang, C. Palmer, M. Zhao, Q. Zhang, Neonicotinoid residues in fruits and
620 vegetables: an integrated dietary exposure assessment approach. *Environ. Sci.*
621 *Technol.* 52(2018), 3175−3184
622 10. Y. Ikenaka, Y. Miyabara, T. Ichise, S. M. M. Nakayama, C. Nimako, M. Ishizuka, C.
623 Tohyama, Exposures of children to neonicotinoids in pine wilt disease control areas.
624 Environ. *Toxicol. Chem.* 38(2019),71-79. doi: 10.1002/etc.4316
625 11. Q. Zhang, Z. Lu, C.H. Chang, C. Yu, X. Wang, C. Lu, Dietary risk of neonicotinoid
626 insecticides through fruit and vegetable consumption in school-age children. *Environ.*
627 *Int.* 126(2019), 672–681. https://doi.org/10.1016/j.envint.2019.02.051
628 12. K. Taira, K. Fujioka, Y. Aoyama, Qualitative Profiling and quantification of
629 neonicotinoid metabolites in human urine by liquid chromatography coupled with
630 mass spectrometry. *PloSone.* 8(2013), e80332.
631 13. J. Ueyama, H. Nomura, T. Kondo, I. Saito, Y. Ito, A. Osaka, M. Kamijima, Biological
632 monitoring method for urinary neonicotinoid insecticides using LC-MS/MS and its
633 application to Japanese adults. *J. Occup. Health.* 56(2014), 461–468
634 14. J. Ueyama, H. K. Harada, A. Koizumi, Y. Sugiura, T. Kondo, I. Saito, M. Kamijima,
635 Temporal level of urinary neonicotinoid and dialkylphosphate concentrations in

636 Japanese women between 1994 and 2011. *Environ. Sci. Technol.* 49(2015), 14522–
637 14528.
638 15. R. Kabata, S. Nanayakkara, S. Senevirathna, K. H. Harada, R. Chandrajith, T. Hitomi,
639 T. Abeysekera, T. Takasuga, and A. Koizumi, Neonicotinoid concentrations in urine
640 from chronic kidney disease patients in north central region of Sri Lanka, J. *Occup.*
641 *Health.* 58(2016),128-133.
642 16. F. Millot, A. Decors, O. Mastain, T. Quintaine, P. Berny, D. Vey, R. Lasseur, E. Bro,
643 Field evidence of bird poisonings by imidacloprid-treated seeds: a review of incidents
644 reported by the French SAGIR network from 1995 to 2014. *Environ. Sci. Pollut. Res.*
645 24(2016), 5469–5485. https://doi.org/10.1007/s11356-016-8272-y
646 17. T. Zhang, S. Song, X. Bai, Y. He, B. Zhang, M. Gui, K. Kannan, S. Lu, Y. Huang,
647 H. Sun, A nationwide survey of urinary concentrations of neonicotinoid insecticides
648 in China. *Environ. Int.* 132(2019), 105114. https://doi.org/10.1016/j.envint.
649 2019.105114
650 18. V. Duzguner, S. Erdogan, Acute oxidant and inflammatory effects of imidacloprid on
651 the mammalian central nervous system and in liver of rats. *Pestic Biochem Phys.*
652 97(2010), 13–18. doi:10.1016/j.pestbp.2009.11.008
653 19. M. Y. Abd-Elhakim, H. H. Mohammed, M. A. W. Mohamed, Imidacloprid Impacts
654 on Neurobehavioral Performance, Oxidative Stress, and Apoptotic Events in the
655 Brain of Adolescent and Adult Rats. *J. Agric. Food Chem.* 66(2018), 13513−13524.
656 doi:10.1021/acs.jafc.8b05793

20. C. Nimako, Y. Ikenaka, Y. Okamatsu-Ogura, J.V. Bariuan, A. Kobayashi, R. Yamazaki, K. Taira, N. Hoshi, T. Hirano, S.M.M. Nakayama, M. Ishizuka, Chronic low-dose exposure to imidacloprid potentiates high fat diet-mediated liver steatosis in C57BL/6J male mice. *J. Vet. Med. Sci.* 83(2021), 487–500, doi: 10.1292/jvms.20-0479.

21. U. Kapoor, M. K. Srivastava, L. P. Srivastava, Toxicological impact of technical imidacloprid on ovarian morphology hormones and antioxidant enzymes in female rats. Food Chem. *Toxicol.* 49(2011), 3086-3089. doi.org/10.1016/j.fct.2011.09.009

22. I. J. Yeh, T. J. Lin, D.Y. Hwang, Acute multiple organ failure with imidacloprid and alcohol ingestion. *Am. J. Emerg. Med.* 28(2020), 255.e1–e3. doi.org/10.1016/j.ajem.2009.05.006

23. O. Klein, W. Karl, Methylene-[14C] Imidacloprid: Metabolism Part of the General Metabolism Study in the Rat. Bayer AG. Leverkusen-Bayerwerk, Germany, (1990), Study No. 87264. DPR Vol. 51950-0021 # 119511.

24. M. Tomizawa, J. E. Casida, Imidacloprid, thiacloprid, and their imine derivatives up-regulate the alpha 4 beta 2 nicotinic acetylcholine receptor in M10 cells. *Toxicol Appl Pharmacol.* 169(2000), 114-20. doi: 10.1006/taap.2000.9057

25. R. Nauen, U. Ebbinghaus-Kintscher, A. Elbert, P. Jeschke, K. Tietjen, Acetylcholine receptors as sites for developing neonicotinoid insecticides. In Biochemical Sites of Insecticide Action and Resistance; Ishaaya, I., Ed. (2001); Springer: New York, 77-105.

679 26. D. Broznic, J. Marini, M. Tota, G. C. Juresic, C. Milin, Kinetic Evaluation of
680 Imidacloprid Degradation in Mice Organs Treated with Olive Oil Polyphenols
681 Extract, Croat. *Chem. Acta.* 81(2008), 203-209.
682 27. M. Tomizawa, J. E. Casida, Desnitro-imidacloprid activates the extracellular signal-
683 regulated kinase cascade via the nicotinic receptor and intracellular calcium
684 mobilization in N1E-115 cells. *Toxicol Appl Pharmacol.* 184(2002), 180-186.
685 28. T. L. Swenson, J. E. Casida, Aldehyde oxidase Importance in vivo in xenobiotic
686 metabolism: Imidacloprid nitroreduction in mice, *Toxicol Sci,* 133(2013), 22–28
687 29. K. H. Harada, K. Tanaka, H. Sakamoto, M. Imanaka, T. Niisoe, T. Hitomi, H.
688 Kobayashi, H. Okuda, S. Inoue, K. Kusakawa, M. Oshima, K. Watanabe, M.
689 Yasojima, T. Takasuga, A. Koizumi, Biological monitoring of human exposure to
690 neonicotinoids using urine samples, and neonicotinoid excretion kinetics. *PLoS One,*
691 11(2016),1–16.
692 30. L. Yang, Q. Shen, T. Zeng, J. Li, W. Li, Y. Wang, Enrichment of imidacloprid and
693 its metabolites in lizards and its toxic effects on gonads. *Environ. Pollut.* 258(2020),
694 113748. https://doi.org/10.1016/j.envpol.2019.113748
695 31. A. K. Ford, E. J. Casida, Chloropyridinyl Neonicotinoid Insecticides: Diverse
696 Molecular Substituents Contribute to Facile Metabolism in Mice. *Chem. Res. Toxicol.*
697 19(2006), 944-951
698 32. N. Schippers, W. Schwack, Photochemistry of Imidacloprid in Model Systems. *J.*
699 *Agric. Food Chem.* 56(2008), 8023–8029.

700 33. M. Tomizawa, N. Zhang, A.K. Durkin, M.M. Olmstead, J.E. Casida, The
701 Neonicotinoid Electronegative Pharmacophore Plays the Crucial Role in the High
702 Affinity and Selectivity for the Drosophila Nicotinic Receptor: An Anomaly for the
703 Nicotinoid Cation-π Interaction Model. *Biochemistry*, 42((2003), 7819 - 7827.
704 34. K. Takahashi, T. Tsurumi, M. Inami, Z. Li, T. Kusakabe, S. Kikkawa, I. Azumaya,
705 N. Tominaga, Y. Ikenaka, K. Arizono, K. Kato, Syntheses of 4-OH and 5-OH
706 Imidacloprids. *Chemistry Select*, 4(2019), 7343 –7345. doi:10.1002/slct.201901491.
707 35. S. Ohno, Y. Ikenaka, K. Onaru, S. Kubo, N. Sakata, T. Hirano, Y. Mantani, T.
708 Yokoyama, K. Takahashi, K. Kato K. Arizono, T. Ichise, S.M.M. Nakayama, M.
709 Ishizuka, N. Hoshi, Quantitative elucidation of maternal-to-fetal transfer of
710 neonicotinoid pesticide clothianidin and its metabolites in mice. *Toxicol. Lett.*
711 322(2020), 32-38. doi: 10.1016/j.toxlet.2020.01.003
712 36. European Commission. SANTE/11813/2019. Analytical quality control and method
713 validation procedures for pesticide residues analysis in food and feed. Implemented
714 by 01/01/2020. Directorate General for Health and Food Safety. Available online:
715 https://ec.europa.eu/food/sites/food/files/plant/docs/pesticides_mrl_guidelines_wrkdoc
716 _2019-12682.pdf. (accessed on 19 March 2021).
717 37. J. Ueyama, A. Arisa, Y. Ueda, N. Oyab, Y. Sugiuraa, Y. Ito, T. Ebara, M.
718 Kamijima, Biomonitoring method for neonicotinoid insecticides in urine of non-
719 toilet-trained children using LC-MS/MS. *Food Addit Contam Part A,* (2020),
720 https://doi.org/10.1080/19440049.2019.1696020

721 38. M. Alzweiri, D. G. Watson, C. Robertson, G. J. Sills, J. A, Parkinson, Comparison
722 of different water-miscible solvents for the preparation of plasma and urine samples
723 in metabolic profiling studies. *Talanta*, 74(2008), 1060–1065.
724 39. T. Ly, T. Ho, P. Behra, T Nhu-Trang, Determination of 400 pesticide residues in
725 green tea leaves by UPLC-MS/MS and GC-MS/MS combined with QuEChERS
726 extraction and mixed-mode SPE clean-up method. *Food Chem.* 326(2020), 126928.
727 https://doi.org/10.1016/j.foodchem.2020.126928
728 40. S. Uclés, A. Lozano, A. Sosa, P. P. Vázquez, A. Valverde, A. R. Fernández-Alba,
729 Matrix interference evaluation employing GC and LC coupled to triple quadrupole
730 tandem mass spectrometry. *Talanta.* 174(2017), 72–81. https://doi.org/10.
731 1016/j.talanta.2017.05.068.
732 41. S. Kittlaus, J. Schimanke, G. Kempe, K. Speer, Assessment of sample cleanup and
733 matrix effects in the pesticide residue analysis of foods using post column infusion
734 in liquid chromatography–tandem mass spectrometry. *J. Chromatogr. A,*
735 1218(2011), 8399–8410. https://doi.org/10.1016/j.chroma.2011.09.054.
736 42. California Environmental Protection Agency (CEPA) (2006). Imidacloprid; Risk
737 characterization document dietary and drinking water exposure.
738 https://www.google.com/url?sa=t&rct=j&q=&esrc=s&source=web&cd=&ved=2ah
739 UKEwjO_pK1m-
740 _vAhVWc3AKHYACDwkQFjAAegQIBRAD&url=https%3A%2F%2Fwww.cdpr.
741 ca.gov%2Fdocs%2Frisk%2Frcd%2Fimidacloprid.pdf&usg=AOvVaw2wFLrnlwK3
742 9QbaYxwrv8YY. [Accessed on November 26, 2020]

743 43. A. D. Schulz-Jander, J. E. Casida, Imidacloprid insecticide metabolism: human
744 cytochrome P450 isozymes differ in selectivity for imidazolidine oxidation versus
745 nitroimine reduction. *Toxicol Lett.* 132(2002), 65–70.
746 44. M. Ospina, L.Y. Wong, S. E. Baker, A. B. Serafim, P. Morales-Agudelo, A. M.
747 Calafat, Exposure to neonicotinoid insecticides in the US general population: Data
748 from the 2015–2016 national health and nutrition examination survey. *Environ. Res.*
749 176(2019), 9. https://doi.org/10.1016/j.envres.2019.108555.
750 45. L. Wang, T. Liu, F. Liu, J. Zhang, Y. Wu, H. Sun, Occurrence and Profile
751 Characteristics of the Pesticide Imidacloprid, Preservative Parabens, and Their
752 Metabolites in Human Urine from Rural and Urban China. Environ. *Sci. Technol.*
753 49(2015), 14633–14640. https://doi.org/10.1021/acs.est.5b04037.
754 46. A. J. Li, M. P. Martinez-Moral, K. Kannan, Variability in urinary neonicotinoid
755 concentrations in single-spot and first-morning void and its association with
756 oxidative stress markers. *Environ. Int.* 135(2020), 9.
757 https://doi.org/10.1016/j.envint.2019.105415.
758 47. A. J. Li, K. Kannan, Profiles of urinary neonicotinoids and dialkylphosphates in
759 populations in nine countries. *Environ. Int.* 145(2020), 106120.
760 https://doi.org/10.1016/j.envint.2020.106120
761 48. A. Wang, G. Mahai, Y. Wan, Z. Yang, Z. He, S. Xu, W. Xia, Assessment of
762 imidacloprid related exposure using imidacloprid-olefin and desnitro-imidacloprid:
763 Neonicotinoid insecticides in human urine in Wuhan, China. Environ. Int. 141(2020),
764 105785. https://doi.org/10.1016/j.envint.2020.105785

765 49. Y. Tao, F. Dong, J. Xu, D. Phung, Q. Liu, R. Li, X. Liu, X. Wu, M. He, Y. Zheng,
766 Characteristics of neonicotinoid imidacloprid in urine following exposure of
767 humans to orchards in China. *Environ. Int.* 132(2019), 105079.
768 https://doi.org/10.1016/j. envint.2019.105079.
769 50. Y. Tao, D. Phung, F. Dong, J. Xu, X. Liu, X. Wu, Q. Liu, M. He, X. Pan, R. Li, Y.
770 Zheng, Urinary monitoring of neonicotinoid imidacloprid exposure to pesticide
771 applicators. *Sci. Total Environ.* 669(2019), 721–728.
772 https://doi.org/10.1016/j.scitotenv. 2019.03.040.

773
774
775
776
777
778
779
780
781
782
783
784

785 **Table 1:** Precision, Freeze-thaw stabilities, Linearity, limit of quantification (LOQ) and Limit of detection (LOD) of the
786 analytical procedure

	Intra-day precision *(%RSDs)*			Inter-day precision *(%RSDs)*	Freeze-thaw Stability *(%RSDs)*		Linearity	LOD (ng/mL)	LOQ (ng/mL)
	2.5 ng/mL	5 ng/mL	10 ng/mL		2.5 ng/mL	10 ng/mL			
IMI	4.7	4.3	3.5	7.8	3.4	9.1	0.999	0.12	0.37
IMI-d4	7.4	6.9	7.4	7.3	4.8	5.6	0.997	***	***
dn-dh-IMI	2.8	4.7	3.7	3.4	23.2	28.6	0.999	0.07	0.22
dn-IMI	4.2	3.6	4.7	4.9	25.9	26.5	0.999	0.06	0.17
IMI-ole	4.0	3.1	5.9	5.6	21.1	16.3	0.999	0.13	0.41
4OH-IMI	6.6	3.3	7.4	7.0	5.8	3.5	0.999	0.28	0.85
5OH-IMI	3.4	3.4	3.9	8.6	0.9	7.2	0.999	0.10	0.29
6-CNA	3.7	4.7	3.5	13.0	29.8	27.2	0.999	0.21	0.64
6-CNA-13C6	3.5	7.7	5.1	10.0	19.5	19.8	0.999	***	***
6-CNA-glycine	5.8	6.9	5.4	9.7	2.8	8.8	0.997	0.47	1.43

787

788

789

790

Fig.1: Metabolic pathways for imidacloprid [5,42].

Fig. 2A&B: (A) Recoveries and, (B) matrix effects of imidacloprid and its metabolites obtained from sample purification with various SPE sorbents. The InertSep SCX cartridge is a silica-based sorbent modified with benzene sulfonyl propyl functional groups; InertSep CBA cartridge is a silica-based sorbent modified with carboxyl ethyl functional groups; InertSep PSA is a silica-based sorbent modified with an ethylene-diamine-N-propyl functional groups; InertSep GC/PSA is a two-layer cartridge, packed with graphite carbon for removing pigments and NH_2 or PSA sorbent for sample cleanup of organic extracts; InertSep Pharma is a copolymer-based sorbent comprised of nitrogen-containing methacrylate and SDB.

Figs. 3A & B: (A) Recoveries and (B) matrix effects of imidacloprid compounds obtained by InertSep CBA purification of various tissue matrices.

Figs. 4*:* Chromatogram showing peaks of imidacloprid and its metabolites in matrix-matched standard working solutions containing all the compounds. Tissue extracts were purified with InertSep CBA. LC Agilent 1290 Infinity Ⅱ, MS: Agilent 6495 Triple Quad LC/MS, Column: Kinetex 1.7µm Biphenyl (2.1×150 mm) (Phenomenex); Mobile phase A: 0.1% Formic acid + 10mM Ammonium acetate in DW, Mobile phase B: 0.1% Formic acid + 10mM Ammonium acetate in MeOH, Flow: 0.35ml/min, Oven: 60℃, gradient: 0-1.5min, B conc 20% -> 1.5-6min, B conc 95% -> 6-7min, B conc 95% -> 7-7.01min, B conc 20% -> 9min end

Fig.5: Bioaccumulations trends of IMI and its metabolites in mice. Figure was plotted from mean contraptions of the target chemicals in mice (n=4). iWAT means inguinal white adipose tissue, mWAT means mesenteric white adipose tissue, gWAT means gonadal adipose tissue.

Fig.6A&B: (A)Tissue-specific accumulation pattern of IMI and its metabolites in mice (Graph was plotted from mean contraptions of the target chemicals in mice, n=4). (B) Sum of mean concentrations of 6 IMI compounds (Σ6 IMI compounds). iWAT means inguinal white adipose tissue, mWAT means mesenteric white adipose tissue, gWAT means gonadal adipose tissue.

Fig. S1: Optimization of SPE elution solvent. Elution efficiencies of solvents were judged based on recoveries of matric-matched standards containing the target IMI compounds. 20% MeOH; 20% methanol in distilled water, 50% MeOH; 50% methanol in distilled water, 20% ACN; 20% acetonitrile in distilled water, 50% ACN; 50% acetonitrile in distilled water.

Fig. S2: Estimation of Method accuracy in three different concentrations (low, medium, and high concentrations of target chemicals).

Fig. S3: Tissue weight effects on the method accuracy (Recoveries and matrix effects of the target chemicals were estimated using three different tissue weights)

832

833

834

835

836

837

Supplementary Data

Table S1: Compound-specific mass spectrometer setting.

Compound	Fragmentor (v)	Collision Energy (eV)	Precursor ion (m/z)	Product ion (m/z)	Retention time (min)
Imidacloprid	380.0	16.0	256.1	175.1	5.3
Imidacloprid-d4	380.0	24.0	260.1	179.1	5.3
4OH-Imidacloprid	380.0	16.0	272.1	191.2	4.6
5OH-Imidacloprid	380.0	20.0	272.1	191.2	4.7
6-Chloronicotinic acid	380.0	20.0	158.0	122.3	3.9
6-Chloronicotinic-13C6	380.0	68.0	164.1	55.0	3.9
6-Chloronicotinic-glycine	380.0	20.0	215.2	169.1	3.5
dn-Imidacloprid	380.0	24.0	211.2	126.1	3.9
dn-dh-Imidacloprid	380.0	20	209.0	126.2	3.7
Imidacloprid-ole	380.0	16	208.2	126.1	4.8

Table S2: Common name, IUPAC names, CAS numbers and molar masses of the target chemicals

Common name	IUPAC name	CAS number	Molar mass (g/mol)
Imidacloprid	1-(6-chloro-3-pyridylmethyl)-N-nitroimi-dazolidin-2-ylideneamine	105827-78-9	255.66
Desnitro-imidacloprid	1-[(6-chloropyridin-3-yl)methyl]imidazolidin-2-imine	-	210.67
Desnitro-dehydro-imidacloprid	N-desnitro-4,5-dehydro-imidacloprid	-	208.67
Imidacloprid-olefin	1-[(6-Chloro-3-pyridinyl)methyl]-N-nitro-1H-imidazol-2-amine	115086-54-9	253.65
4OH-imidacloprid	4-hydroxy-imidacloprid	-	271.66
5OH-imidacloprid	5-hydroxy-imidacloprid	-	271.66
6-CNA	6-Chloronicotinic acid	5326-23-8	157.55
6-CNA-glycine	6-chloronichotinic acid-glycine	-	214.55

- Not applicable

Table S3: Mean concentrations of (ng/g or ng/mL) or imidacloprid and its metabolites in mice tissues (n=4)

	Pancreas	Liver	mWAT	gWAT	iWAT	Lung	Kidney	Brain	Testis	Blood
Imidacloprid	BDL	0.06±0.01	0.54±0.20	1.10±0.10	1.47±0.25	2.30±0.41	1.70±0.43	3.38±1.15	3.73±0.69	3.69±0.67
dh-dn-Imidacloprid	0.02±0.00	0.12±0.04	0.03±0.00	0.02±0.00	0.03±0.01	0.10±0.07	0.05±0.01	0.03±0.01	0.06±0.05	0.03±0.00
dn-Imidacloprid	0.04±0.01	0.31±0.02	0.08±0.01	0.06±0.01	0.13±0.02	0.22±0.17	0.21±0.04	0.26±0.17	0.24±0.04	0.17±0.04
Imidacloprid-olefin	BDL	BDL	0.62±0.15	0.64±0.13	1.44±0.41	0.04±0.00	0.97±0.37	0.71±0.10	2.69±0.58	4.60±0.69
4OH-Imidacloprid	0.10±0.00	BDL	0.36±0.02	0.21±0.02	0.35±0,08	0.28±0.05	1.33±0.30	0.28±0.09	0.60±0.20	1.10±0.28
5OH-Imidacloprid	0.02±0.00	0.02±0.00	0.05±0.02	0.04±0.02	0.10±0.02	0.83±0.19	0.17±0.00	0.06±0.03	0.27±0.10	0.21±0.05

mWAT; mesenteric white adipose tissue
gWAT; gonadal white adipose tissue
iWAT; inguinal white adipose tissue
BDL: below detection limit

Simultaneous Quantification of Imidacloprid and its Metabolites in Tissues of Mice upon Chronic Low-dose Administration of Imidacloprid

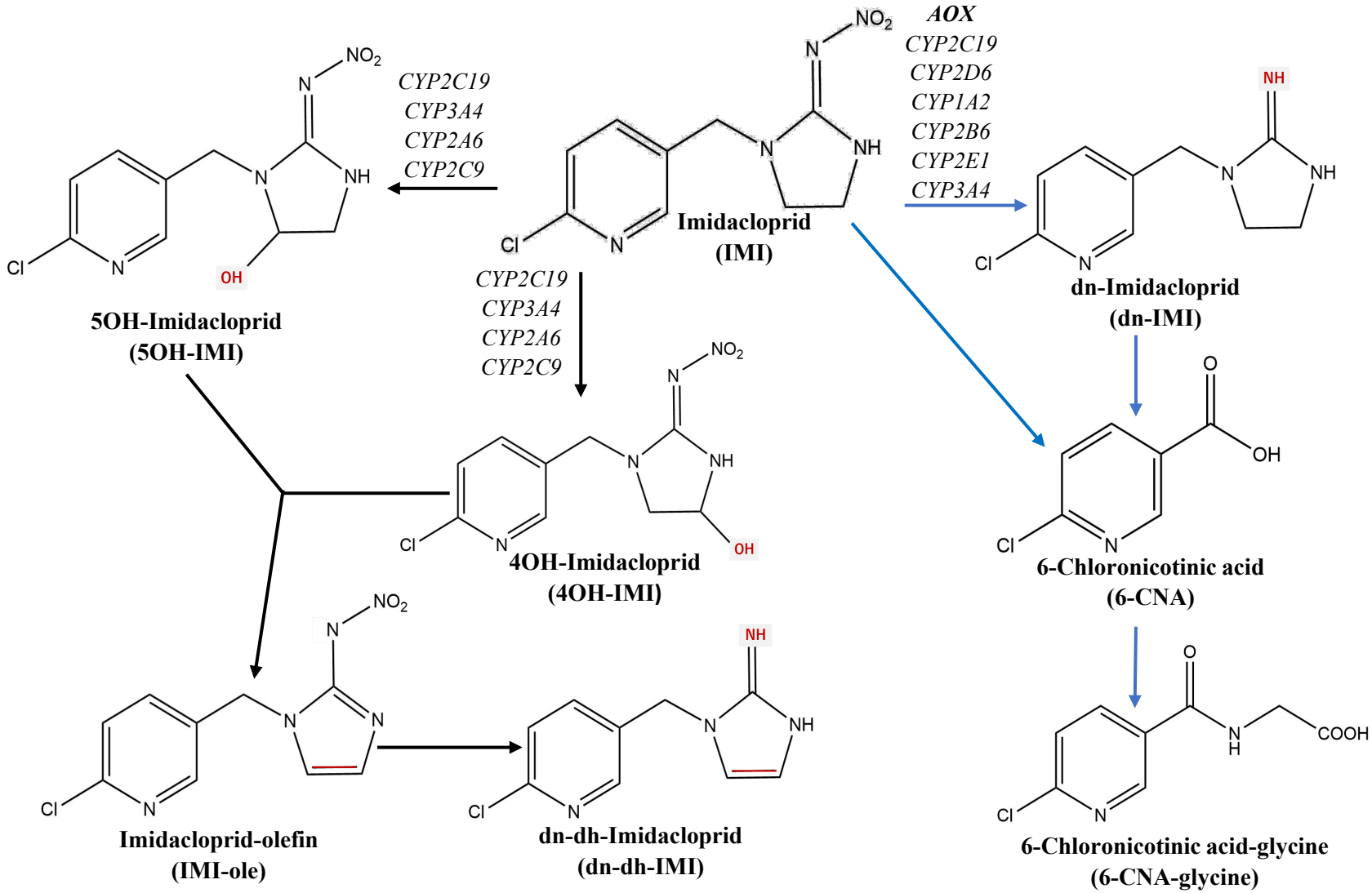
AOX
CYP2C19
CYP2D6
CYP1A2
CYP2B6
CYP2E1
CYP3A4
CYP2C19
CYP3A4
CYP2A6
CYP2C9
CYP2C19
CYP3A4
CYP2A6
CYP2C9
Imidacloprid
(IMI)
5OH-Imidacloprid
(5OH-IMI)
dn-Imidacloprid
(dn-IMI)
4OH-Imidacloprid
(4OH-IMI)
6-Chloronicotinic acid
(6-CNA)
Imidacloprid-olefin
(IMI-ole)
dn-dh-Imidacloprid
(dn-dh-IMI)
6-Chloronicotinic acid-glycine
(6-CNA-glycine)

Fig.1

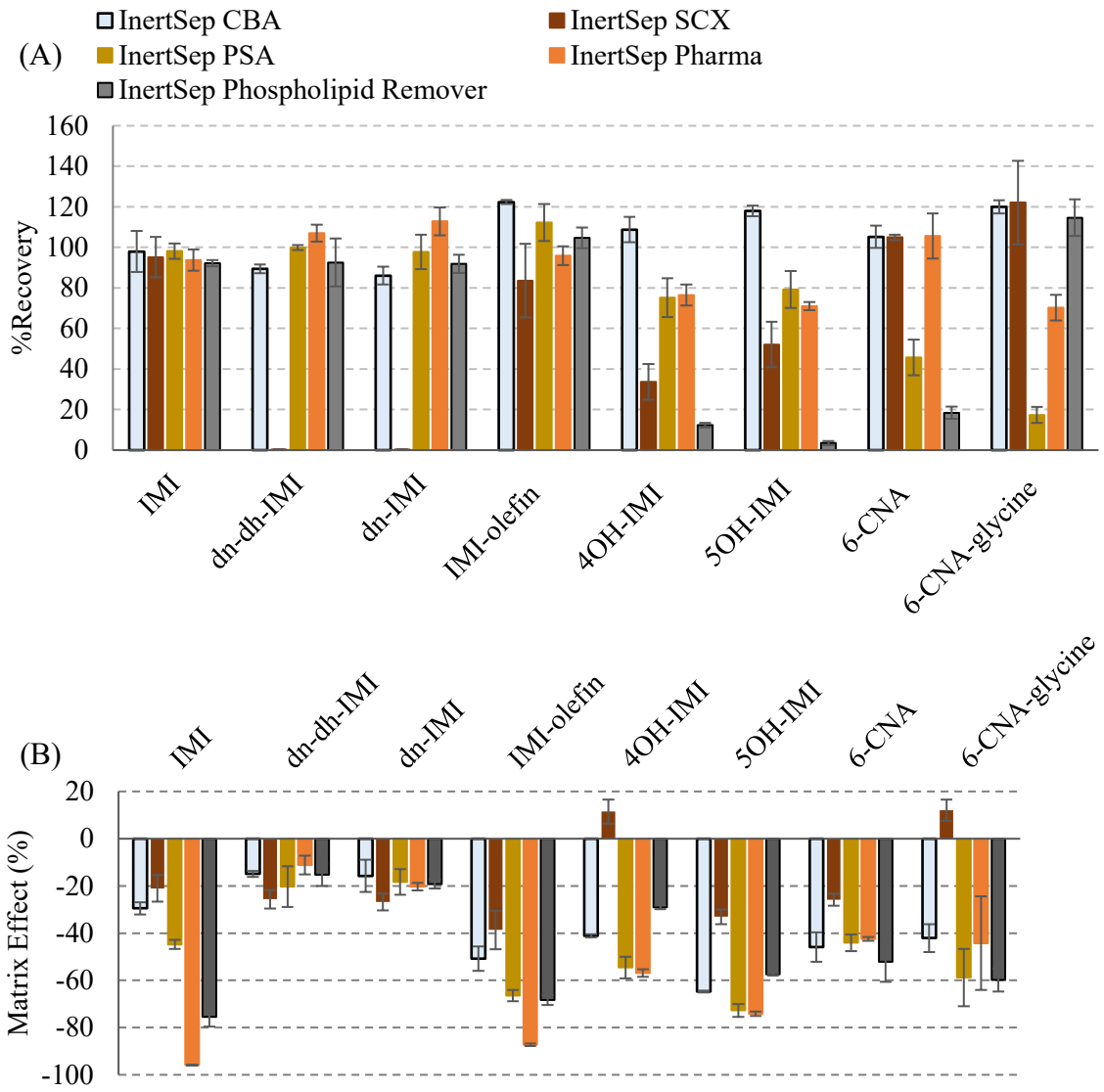
(A)
InertSep CBA
InertSep SCX
InertSep PSA
InertSep Pharma
InertSep Phospholipid Remover
%Recovery
160
140
120
100
80
60
40
20
0
IMI
dn-dh-IMI
dn-IMI
IMI-olefin
4OH-IMI
5OH-IMI
6-CNA
6-CNA-glycine
(B)
Matrix Effect (%)
20
0
-20
-40
-60
-80
-100

Fig.2 A&B

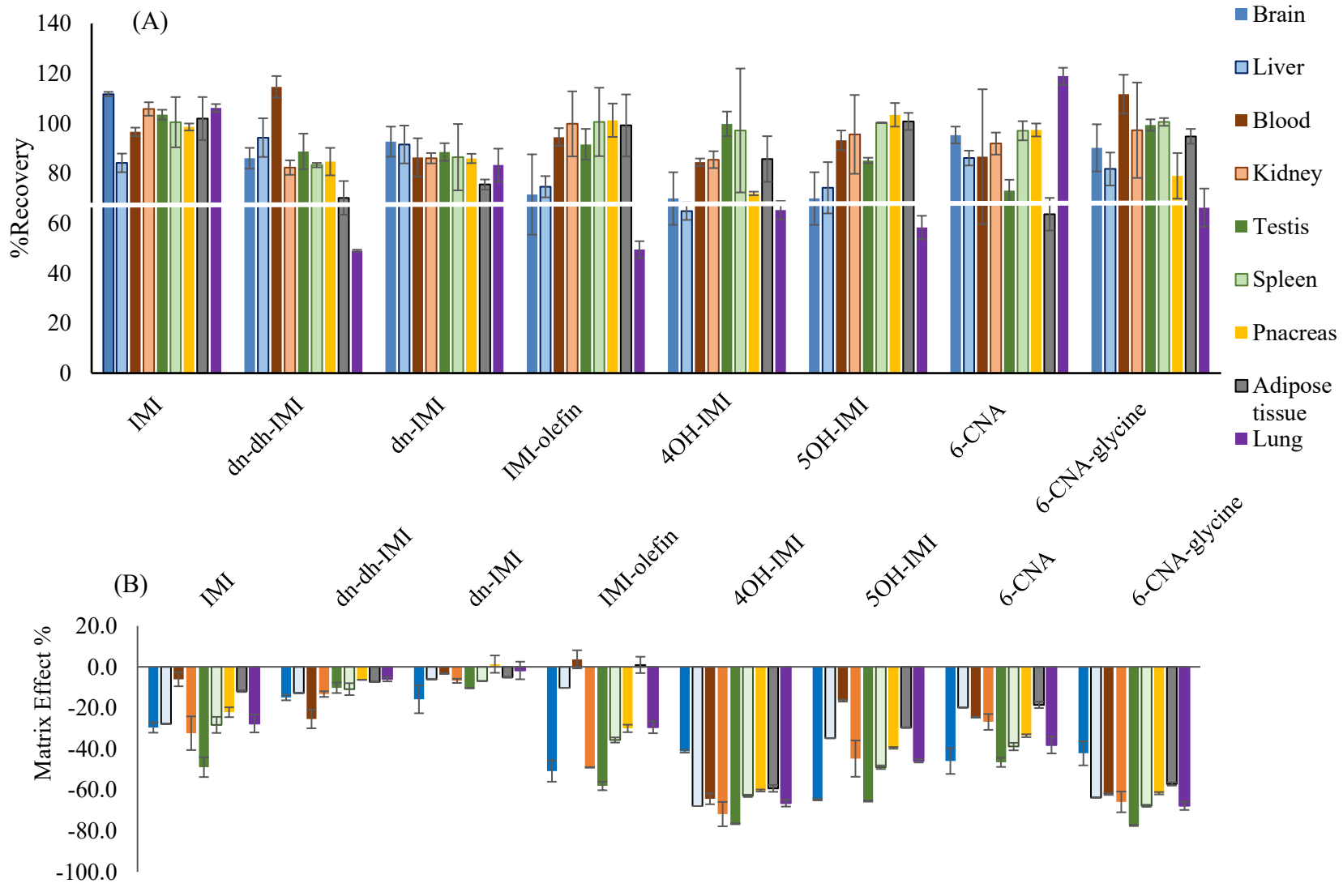
(A)
%Recovery
140
120
100
80
60
40
20
0
IMI
dn-dh-IMI
dn-IMI
IMI-olefin
4OH-IMI
5OH-IMI
6-CNA
6-CNA-glycine
Brain
Liver
Blood
Kidney
Testis
Spleen
Pnacreas
Adipose tissue
Lung
(B)
Matrix Effect %
20.0
0.0
-20.0
-40.0
-60.0
-80.0
-100.0
IMI
dn-dh-IMI
dn-IMI
IMI-olefin
4OH-IMI
5OH-IMI
6-CNA
6-CNA-glycine

Fig.3 A & B

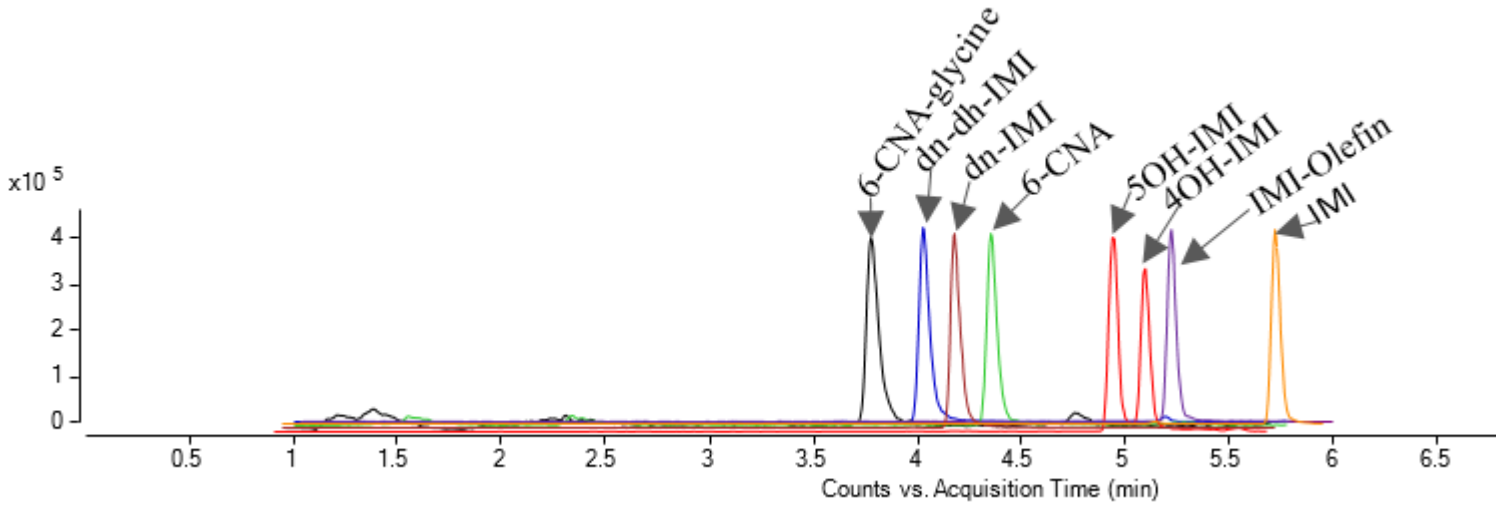
x10 5
4
3
2
1
0
0.5
1
1.5
2
2.5
3
3.5
4
4.5
5
5.5
6
6.5
Counts vs. Acquisition Time (min)
6-CNA-glycine
dn-dh-IMI
dn-IMI
6-CNA
5OH-IMI
4OH-IMI
IMI-Olefin
IMI

Figs. 4

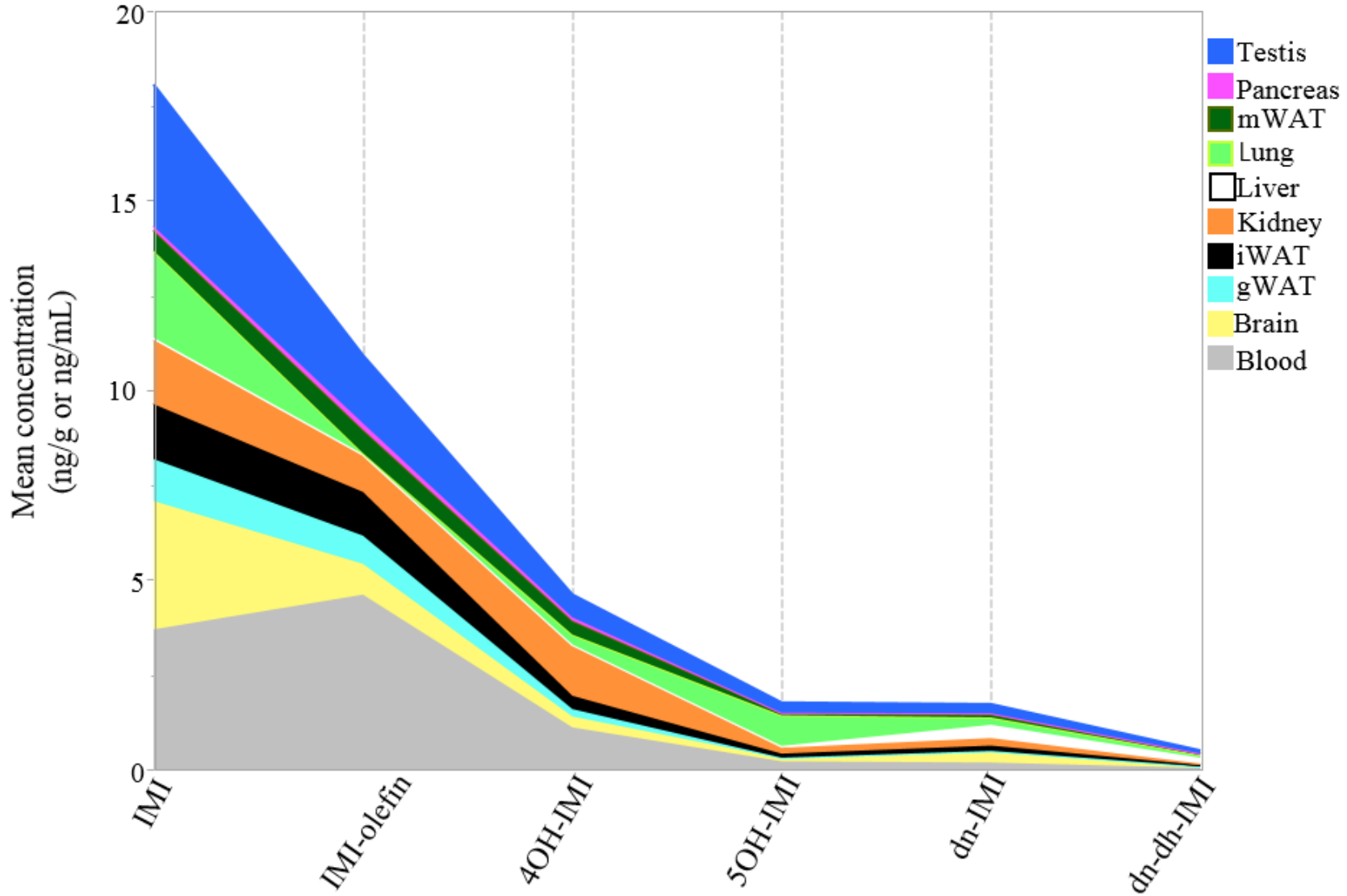
Mean concentration
(ng/g or ng/mL)
20
15
10
5
0
IMI
IMI-olefin
4OH-IMI
5OH-IMI
dn-IMI
dn-dh-IMI
Testis
Pancreas
mWAT
Lung
Liver
Kidney
iWAT
gWAT
Brain
Blood

Fig. 5

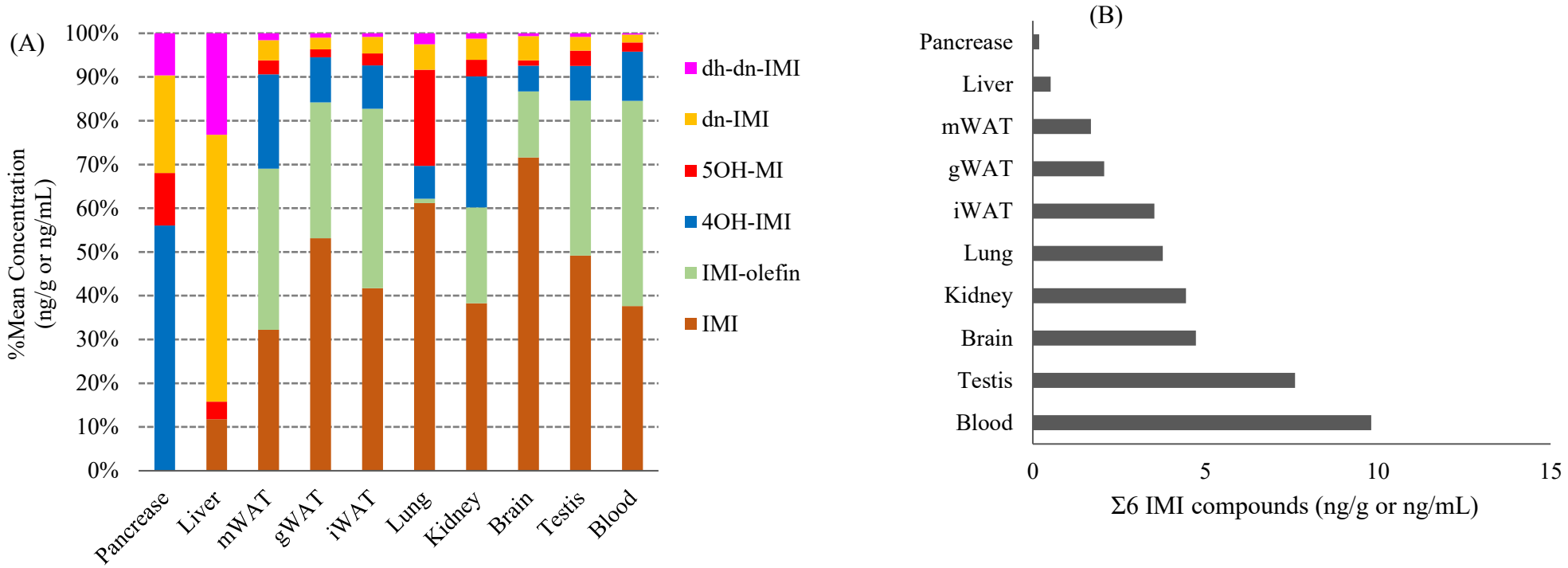
(A)
100%
90%
80%
70%
60%
50%
40%
30%
20%
10%
0%
%Mean Concentration (ng/g or ng/mL)
dh-dn-IMI
dn-IMI
5OH-MI
4OH-IMI
IMI-olefin
IMI
Pancrease
Liver
mWAT
gWAT
iWAT
Lung
Kidney
Brain
Testis
Blood
(B)
Pancrease
Liver
mWAT
gWAT
iWAT
Lung
Kidney
Brain
Testis
Blood
0
5
10
15
Σ6 IMI compounds (ng/g or ng/mL)

Fig.6 A&B